LA-UR-21-29366
Approved for public release; distribution is unlimited.

Title: Vessels Irradiation Experimental Campaign

Author(s): Marcath, Matthew James
Mayo, Douglas R.
Meierbachtol, Krista Cruse
Klain, Kimberly L.
Gonzales, Samuel M.
Engeman, Scott Alan
Mclean, Thomas Donaldson
McClanahan, Tucker Caden

Intended for: Report

Issued: 2021-11-16 (rev.1)

Vessels Irradiation Experimental Campaign

Tucker C. McClanahan, Matthew J. Marcath, Douglas R. Mayo, Krista C. Meierbachtol, Kimberly L. Klain, Samuel M. Gonzales, Scott A. Engeman, Thomas McLean

Table of Contents

1 Introduction

Radiation transport calculations are often used to estimate dose or exposure to components and personnel surrounding a radiation source. The radiation sources for these calculations are decaying radionuclides within various nuclear materials. Under long-term radiation exposure, some components may show signs of material damage such as hardening, cracking, discoloration, etc. resulting from the dose received from nearby radioactive sources. Radiation dose quantities are a useful means to correlate material damage or degradation to radiation interactions. The degradation is dependent on how incident radiation interacts and deposits energy into the material.

The purpose of this report is to document the neutron flux field characterization experiments and to provide experiment data to validate radiation transport models. To predict material damage, irradiation experiments expose materials to known radiation fields to correlate the exposure to damage effects. As a part of irradiation experiments, the neutron field in the experiment must be well characterized; this characterization includes effects like room return. Only the neutron component of the ^{252}Cf sources is considered in theses measurements and calculations.

The neutron field characterization experiments used a wide variety of detectors to measure the incident neutron-energy spectra at the sample location. It is not feasible to directly measure the dose to sample materials, necessitating complementary measurements and calculations of the radiation field. A discussion of the spectrometer best practices and the data post-processing is included in this report.

The Monte Carlo particle transport code, Monte Carlo N-Particle (MCNP) Version 6.2.1, model of the neutron field and experiment geometry was validated with the experiment data. A detailed discussion of the MCNP calculations is included in Reference [1]. The validated MCNP model of the neutron field and experiment geometry can be used to calculate different dose responses to samples. Also, the MCNP results are also used to help interpret trends in the measured data.

2 Facility Overview

The neutron field used for sample irradiation is impacted by the laboratory environment and the material sample surroundings. The facility structure was considered because it can contribute significantly to the neutron room return at the sample location. The irradiation experiment facility is shown in Figure 1, where the view of the facility is a plan view sliced at the height of the source. The facility has 1-m-thick concrete walls, floor, and ceiling along with a 15.24-cm-thick stainless-steel sliding door. The entrance to the facility is a maze as shown in Figure 1. The experiment is positioned in the middle of the irradiation room in the models and is approximately in the center of the room for the measurements.

Figure 1 shows the stainless-steel vessels containing the material of interest located 25 cm from the source and the spectrometers surrounding the ring of vessels located 50 cm from the source. The whole facility is included in the MCNP models in order to account for the room return component of the neutron flux at the detector location. Room return is the component of the neutron flux that is a result of the neutrons scattering off of the walls, floor, ceiling, table, etc., and then interacting within the detector or material of interest.

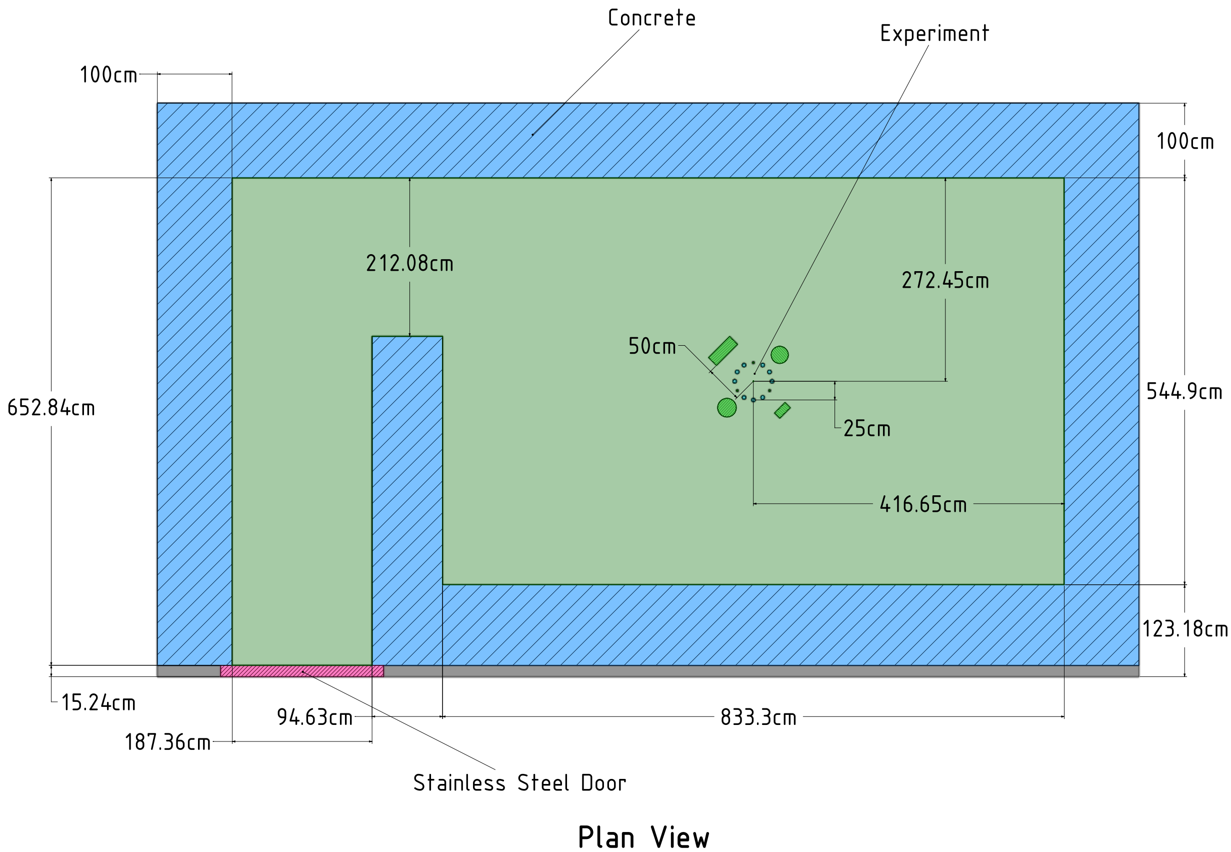

Figure 1: Facility and experiment bottom-up plan view showing the overall scale of the facility and the materials used to define the facility.

Figure 2 shows the overall dimensions of the facility. The room is a little over 500 cm in height with 100 cm floor, ceiling, and walls.

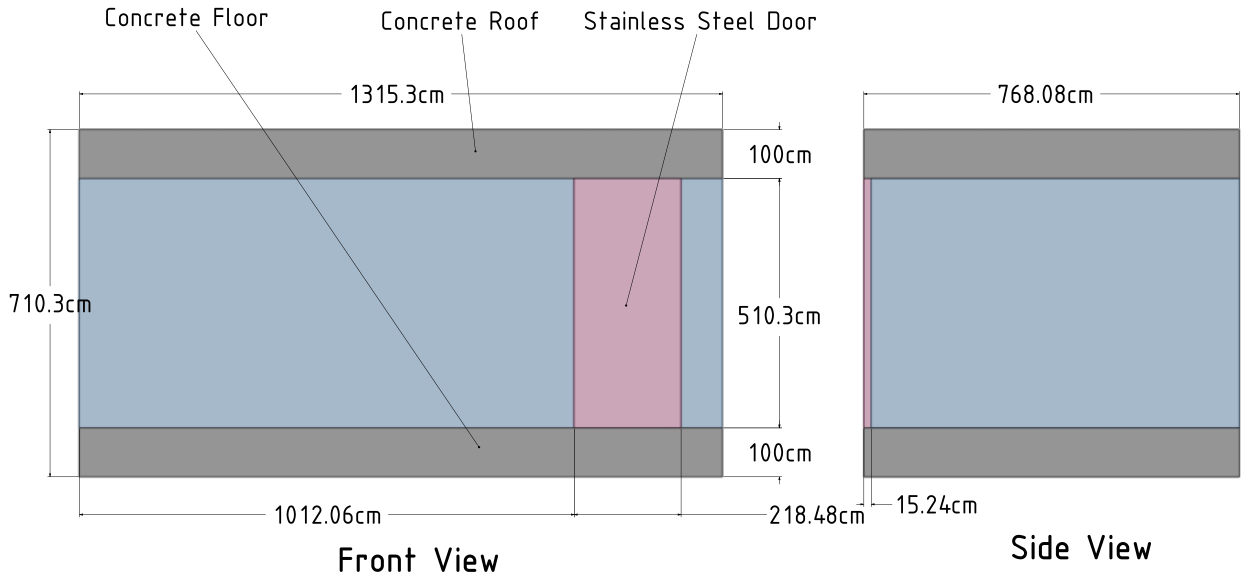

Figure 2: Side view of the facility showing the steel sliding door and dimensions.

3 Experimental Setup

Various radiation detection systems and analyses were used to characterize the neutron field incident on the samples. Two types of sample vessels are present in the material irradiation experiments: nine Swagelok 304-05SF4-150 vessels and three Kurt J. Lesker Company FN-0311 ConFlats. The Swagelok vessels are filled with 150 ml of polyethylene and the ConFlats are filled with 15 ml of polyethylene. Figure 3 shows the layout of the vessels, the ConFlats, and the detectors around the source. The aluminum table and stabilization rails are also included in the model. The vessels and ConFlats are uniformly positioned at a radius where the center of mass of the vessel or Conflat were 25 cm from the source. The vertical position of the vessels or ConFlats were adjusted with jack-stands to align the sample's center of masses with the source. The spectrometers are positioned in a similar fashion except the radius is 50 cm.

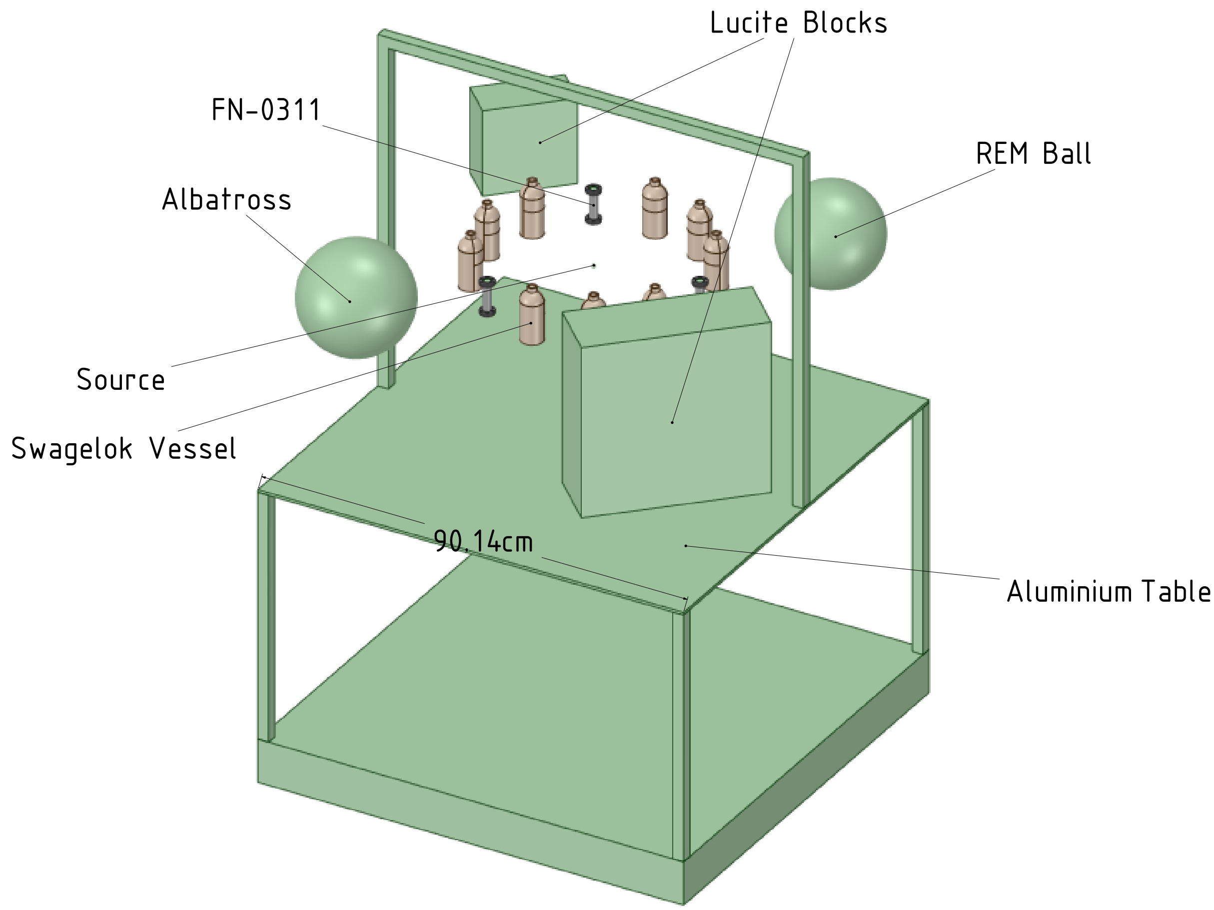

Figure 3: Vessels and detectors idealistic arrangement around source and may not match the experimental layout exactly.

The experimental setup described was exposed to several irradiations using two ^{252}Cf sources; some irradiations used one or both sources stacked on top of each other. The irradiation lengths varied from 20 minutes to multiple days.

3.1 Rotating Neutron Spectrometer

A variety of detectors are used in the irradiation experiments to characterize the source. The Rotating Neutron Spectrometer (ROSPEC) by Bubble Technology Industries uses proton recoil counters and the resulting pulse height data to measure neutron energies [2, 3]. The ROSPEC consists of four spherical gas-filled proportional counters to measure 50 keV to 4.5 MeV neutrons and two ^{3}He detectors to measure thermal and epi-thermal neutrons. These six detectors sit on a rotating platform and provide neutron flux energy spectra to the user. Appendix B contains documentation from Thomas McLean on the mechanics of the ROSPEC unfolding algorithm.

3.2 Bonner Sphere

A multi-sphere, or Bonner sphere, neutron spectroscopy system (MSS) is also used in the irradiation experiments as another measurement of the neutron flux energy spectrum [4]. The MSS consists of ten polyethylene spheres of varying radii from 3 to 12 inches with a ^{3}He proportional counter in the middle of each sphere. The number of pulses in each detector is proportional to the number of thermal neutrons interacting in the detector and a pulse height distribution is produced in each sphere. The response functions of each sphere are incorporated into the MSS unfolding code along with the pulse height distributions to produce a neutron flux energy spectrum. LANL-specific instructions for setup and measurements using the LANL MSS set are included in Appendix C.

3.3 Bubble Detector Spectrometer

The Bubble Detector Spectrometer is a passive neutron detector set that measures neutron dose for a given energy range by counting the bubbles generated in the detector from an exposure [5, 6]. The Bubble Detector Spectrometer tubes measure a coarse energy spectrum. The bubbles are formed in the detector material by the neutron interacting in the superheated detector material and generating a gas bubble. The bubbles are then counted either by hand or by machine and the number of bubbles can then be converted in to total tissue dose using the bubble detectors efficiency. Each bubble detector is sensitive to a specific neutron energy range. The number of bubbles in each spectrometer tube is used as input to the Unfolding of Bubble Technology Bubble Detector Spect Set unfolding spreadsheet. The spreadsheet output is a coarsely binned, neutron-flux energy spectrum.

3.4 Other Instruments

Other detectors were present to measure neutron dose 50 cm from the source location. Those instruments included the ALBATROSS HPI2080 Pulsed Neutron REM Meter, REMBall, thermoluminescent dosimeters (TLDs), and Shielded Neutron Assay Probe (SNAP) [7, 8, 9]. The ALBATROSS was set to integrate mode and used to measure the tissue dose over the entire irradiation period. The SNAP measured the total neutron count rate over the irradiation period to measure the source strength. Data taken with these instruments will not be discussed in this report.

4 MCNP Modeling

This section details the MCNP6 modeling of the experimental setup described above. The MCNP model of the neutron field and experiment geometry will be validated with the experiment data. The validated MCNP model can be used to help interpret trends in the measured data and can be used in future work to calculate different dose responses to samples.

Section 4.1 discusses the geometry and materials used in the MCNP models. Section 4.2 details the source used in the MCNP calculations and how the source strength is calculated. Section 4.3 gives reference to the report that details the tallies used to calculate silicon equivalent dose and provides additional details on the tallies used not covered in the aforementioned report.

4.1 Geometry and Materials

The MCNP6 models use a CSG representation of the geometry shown in Figures 1, 2, and 3. The full details of Figures 1, 2, and 3 are captured by the CSG geometry. The authors chose CSG as the geometry representation rather than an unstructured mesh because of issues experienced when using an unstructured mesh and point detector tallies in the same input deck. The results of the point detector tallies when using unstructured mesh produced non-realistic neutron energy-differential flux spectra, whereas the results using CSG produced reasonable neutron spectra at the detector locations. The composition and density of the materials used in the MCNP6 models are from the material compendium [10]. The model used ordinary concrete defined by the National Institute of Standards and Technology. For this work, $S(\alpha,\beta)$ tables were not included in the material models.

4.2 Source

An ideal Cf-252 source was used in the calculations; the source only produced spontaneous fission neutrons. The ^{252}Cf source rate was modeled after source ID 43804B, NS6227, RSSDMS 1452 with original activity of 2.7E4 μCi on 10/01/2010. The source spectrum used in the calculations is shown in Figure 4. This original activity was decayed to the time of measurement and converted into n/s using Equation 1, where $\phi = 7.3071E6$ n/s is the neutron emission rate at the time of measurement, $A_0 = 9.99E8$ Bq is the original activity, $B_{SF} = 0.0309$ is the spontaneous fission branching ratio, $\nu = 3.7692$ neutrons/fission, $\lambda = 0.26206$ 1/years is the ^{252}Cf decay constant, and $t = 10.5616$ years is the time difference between time of measurement and the date of original activity.

$$\phi = A_0 B_{SF} \nu \exp(-\lambda t) \tag{1}$$

Equation 2 shows the Maxwellian Fission Spectrum equation where $a = 1.18$ and $b = 1.03419$, $p(E)$ is the probability function, E is energy in units of MeV, and ϕ is the neutron emission rate calculated by Equation 1 used to scale the probability density function in MCNP. The ϕ parameter is used as the `wgt` in the `sdef` nh card in the MCNP input deck.

$$p(E) = \phi \exp(-E/a) \sinh((bE)^{1/2}) \tag{2}$$

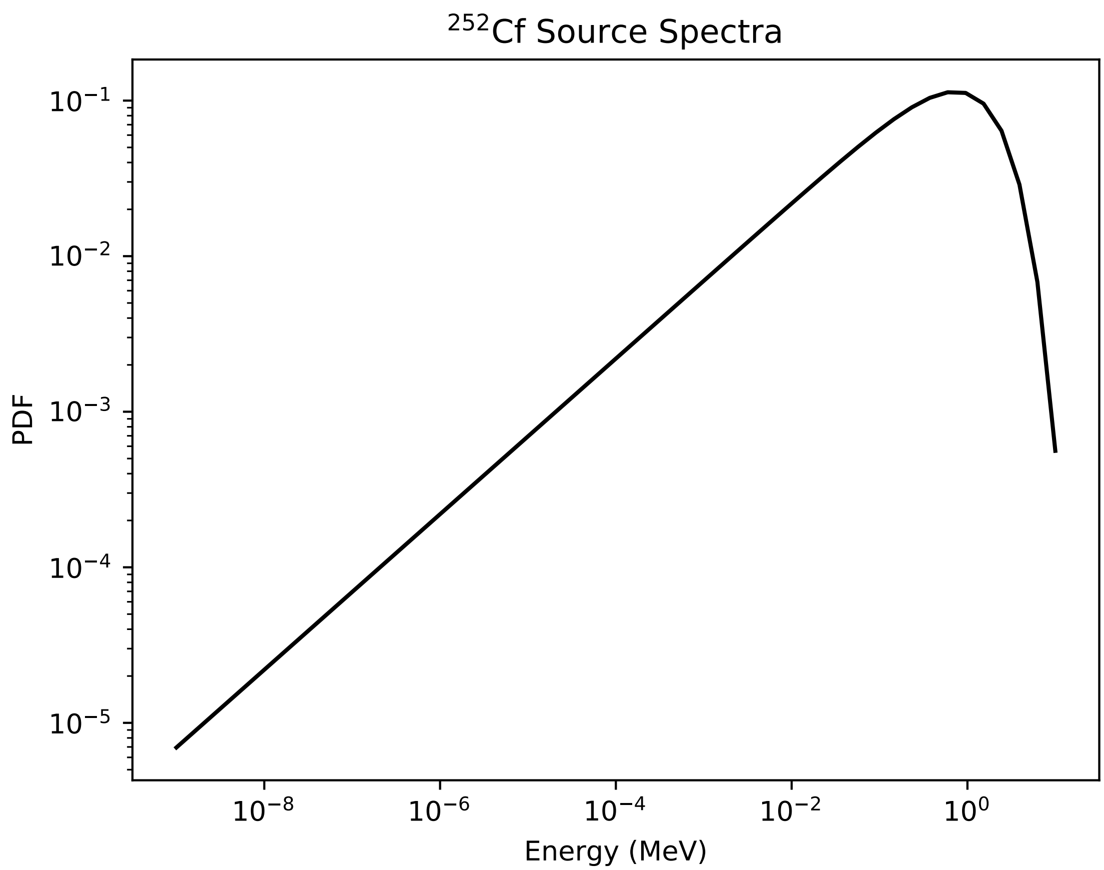

Figure 4: ^{252}Cf spontaneous fission neutron spectrum probability distribution.

Only the neutron emission component of the ^{252}Cf source is considered in the MCNP calculations and measurements. The photon emission component has been evaluated with other experiments. In the future, the source should be shielded to ensure the photon component does not contribute to the measurements.

4.3 Tallies

Several tally types are used in the MCNP model to calculate various quantities of interest. Volume-averaged flux tallies in the vessels and ConFlats were calculated using an F4 tally, following the methodology for calculating silicon equivalent dose in McClanahan's report [1].

In order to characterize the room return, a F5 point detector tally modified with a FT ICD tally treatment card that identifies the cell from which each detector score was specified. A FU special tally was used in conjunction with the F5 tally to provide the cells of interest and provide their corresponding bins. The result of this tally is the flux at the point detector location binned by the cell where the history last interacted. This interaction may be a source, scattering or other reaction generating a neutron event. The cell flagging, CF, card may be used to characterize whether or not a history came from a group of cells but does not provide the details of which cell the history came from. Tally tagging is another method of determining the particle's origins but it does not account for the cell where the particle last interacted. Below is a snippet of the MCNP6 input deck where the F5 tally with the FT ICD tally treatment card is applied.

```
F5:n 0 -25 0 0.5
E5 1E-9 50ilog 20
FT5 ICD
FU5
      100 $ Concrete Walls
      102 $ Room Air
      103 $ Floor
      104 $ Roof
      105 $ Pneumatic Door
      201 $ Vessel Steel
      202 $ Air Fill
      203 $ Vessel Fill
      313 $ fn-0133 fill
      500 $ Source
```

5 Results

This section shows results from the measurements with the various detectors and the MCNP calculations used to inform the experimental setup. The measured spectra shown in this section have been processed by each of the detector's respective unfolding algorithms. The calculated spectra are a result of point detector tallies in MCNP and not a simulated detector response. The point detector tallies do not account for the detector efficiency nor the detector characteristics. Many of the figures allow for direct comparison of the measured spectra with the calculated spectra and in many cases, the agreement is strong.

After several irradiation periods with various instruments, the energy differential neutron flux was measured. Figure 5 shows the measured and calculated neutron flux at 50 cm from the source, and shows fair agreement between the measured and calculated values. The data plotted in lethargy space can be found in Appendix A. The ROSPEC unfolded flux shows a non-physical discontinuity at roughly 0.06 and 0.120 MeV, but is otherwise as expected. The Bubble Tech unfolded spectrum did not produce results below 0.6 MeV. This agreement demonstrates the MCNP model adequately replicates the neutron field near the samples. The measured energy-integrated neutron flux values agree with the calculated value to within 5% with the ROSPEC data and 12% with the Bonner Sphere data. Overall, the measurement is consistent with the simulation in both spectral shape and intensity. The measurements are also consistent with each other. The energy-integrated neutron flux value for the Bubble Tech Average data is disregarded because of the lack of reliable data in the low-energy region.

The Bubble Tech Average dataset is an average of independent measurements with the Bubble Tech Spectrometer set. Six bubble detectors for a given energy range were irradiated, read, averaged, and then unfolding was performed. The variance in counting bubbles using the optical readout was large and errors associated with collecting data from the Bubble Tech Spectrometer tubes were too high to be a reliable means of determining the neutron energy spectrum. The data is collected from the Bubble Tech tubes by optically counting bubbles by an automatic computer-driven system [5]. The number of bubbles counted by the automatic system varies significantly when the tube is rotated. The authors also found that for the given source strength, too few bubbles were produced in the lowest sensitivity tubes to be a reliable form of measurement for the experimental setup.

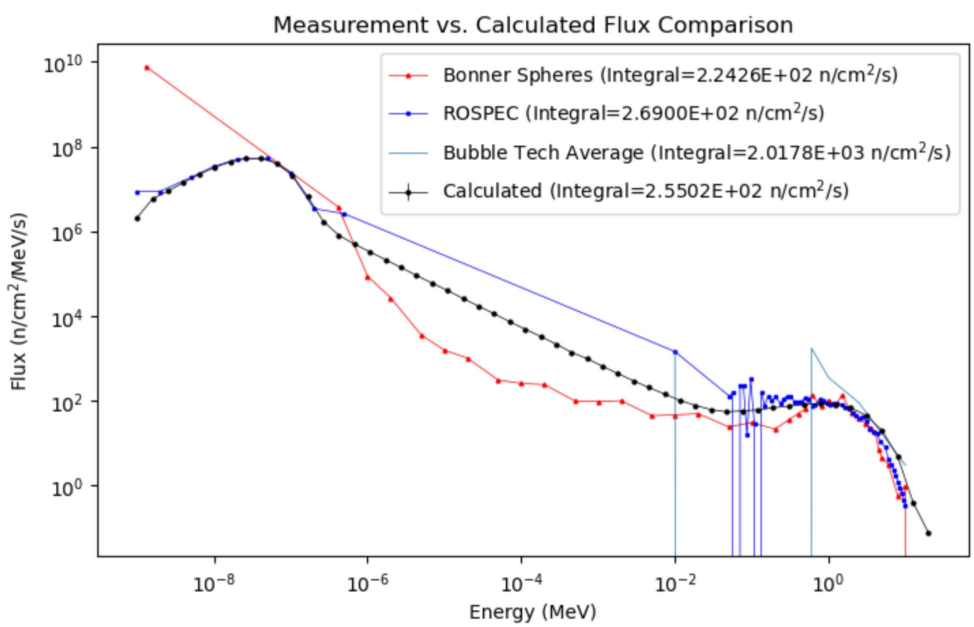

Figure 5: Measured and calculated energy differential neutron flux comparison at 50 cm from the source. Errorbars are not shown.

To highlight the energy regimes where the measurement differs from the calculated values, Figure 6 shows the ratio of measured to calculated neutron flux. The ROSPEC spectrum matches with the calculated spectrum at the low- and high-energy regions, but the intermediate-energy regime is significantly different than the calculation. The differences observed in the low-energy region of the Bonner sphere spectrum and the intermediate-region of the ROSPEC spectrum are a result of a combination of lack of data and the interpolation scheme used to compute the ratios. The ROSPEC has few data points in the intermediate energy range and the Bonner spheres have few data points below 1 eV. Figure 6 provides estimates of uncertainty without simulating the detector response in MCNP.

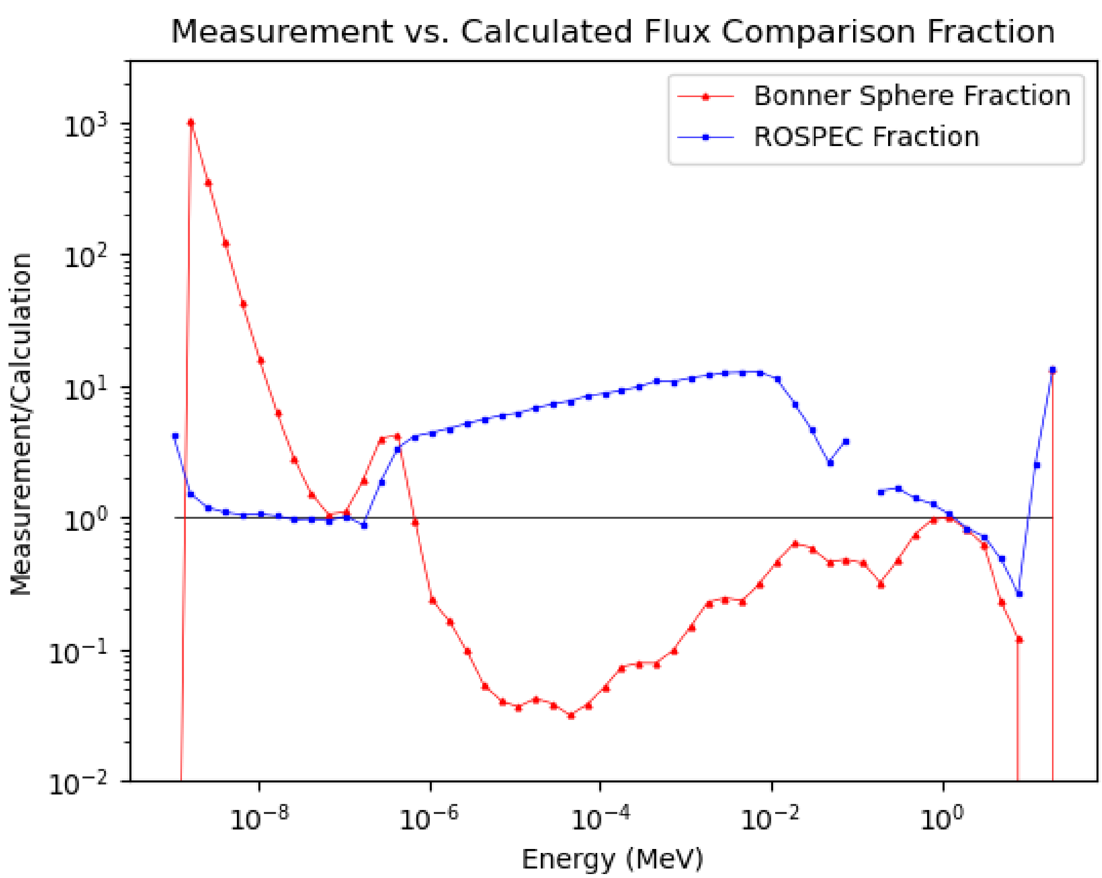

Figure 6: Ratio plot of measured over calculated neutron flux. The measured spectra were interpolated logarithmically to compare to the calculated flux.

The ROSPEC and Bonner Sphere measurement systems must be placed a minimum of 50 cm from the source in order to validate the assumptions in the unfolding algorithms. Figure 7 shows the measured spectra for the detectors located at 25 and 50 cm. The shapes of the two spectra at 25 and 50 cm from the source for a given instrument are significantly different. The resulting spectra from a misplaced detector have the potential to include significant errors introduced by the unfolding algorithm.

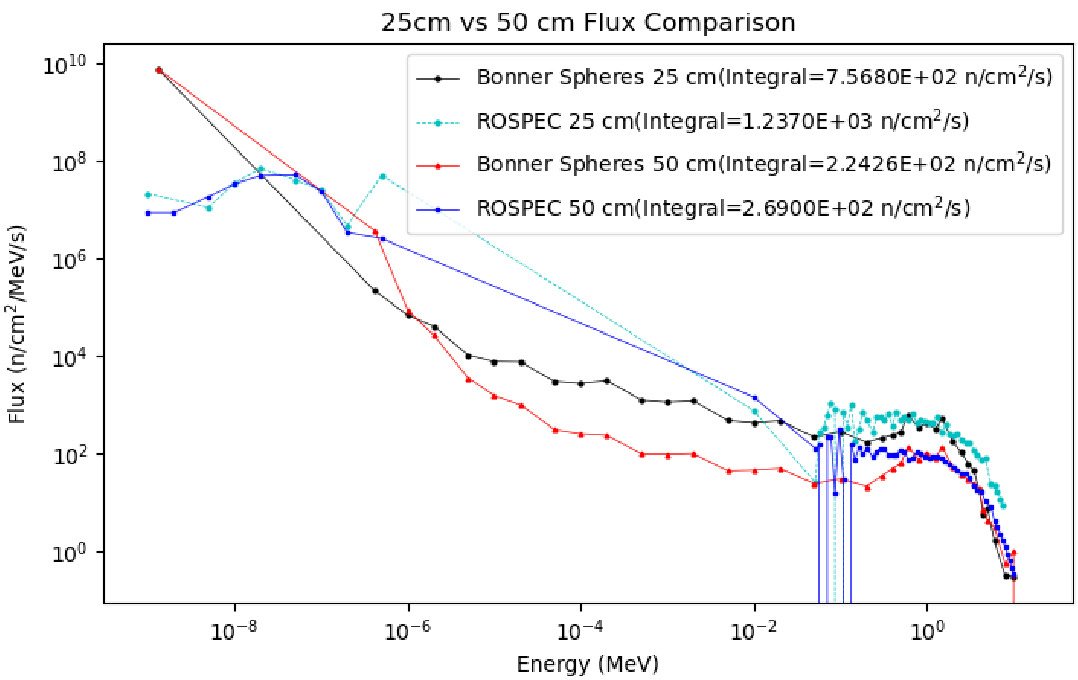

Figure 7: Comparison of detectors located 25 cm and 50 cm from source.

A F5 point detector tally modified with a FT ICD tally treatment card was used to identify the various contributors to the neutron flux at the sample location. The contributions to the neutron flux located 25 cm from the source are shown in Figure 8. The high-energy component of the total neutron flux is dominated by neutrons directly from the source. In the intermediate energy region, neutrons scattering from the steel vessel dominate. The thermal peak of the total neutron flux is dominated by the contributions from the concrete walls. The roof and air contribute the least to the overall neutron flux. Modeling the room return component of the incident neutron flux spectrum is key to accurately calculating dose to the sample. The Watt dataset shown in Figure 8 is an idealized source contribution to the detector and is not a result from the MCNP calculations. The dataset labeled "Source" and "Watt" are direct contributions from the source and should be exactly the same if enough histories were sampled by MCNP.

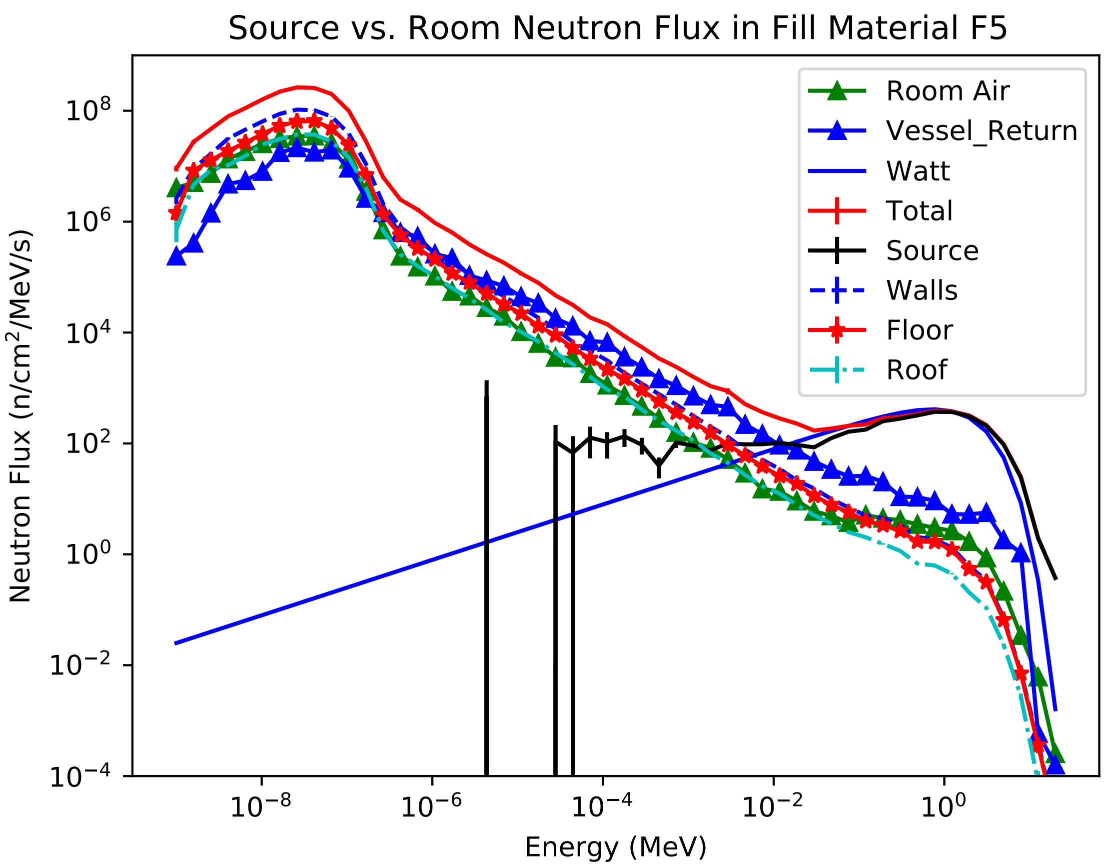

Figure 8: Contributions to neutron flux at the sample location.

6 Conclusions

This report documents the neutron flux field characterization experiments and to provides validation of radiation transport models of the source and environment. The neutron field characterization experiments used the ROSPEC, Bonner spheres, and Bubble Tech Spectrometer to measure the incident neutron energy spectra at the sample location. The variance in the Bubble Tech Spectrometer response was large and found to be unsuitable for this application. The MCNP model of the neutron field and experiment geometry produced energy-differential neutron flux spectra that agree well with experiment data.

The MCNP modeling methodology used to identify various scattering sources of the specific facility are discussed and quantified. Neutrons scattering from the concrete walls contribute the most in the thermal region of the neutron flux at 25 cm from the source and neutrons directly from the source dominate the high-energy region of the neutron flux. Future work includes shielding the ^{252}Cf source with tungsten or lead to attenuate the gamma-ray emissions from the source to reduce the gamma-ray contribution to the dose in the materials of interest. Also, future work should study the impact of $S(\alpha,\beta)$ tables on the calculation result.

References

[1] T. McClanahan, M. Marcath, and D. Mayo, "Silicon-equivalent dose estimations," tech. rep., LANL, 2021.

[2] Bubble Technology Industries, *ROtating neutron SPECtrometer*, 2011.

[3] T. D. McLean and R. T. Devine, "Rospec measurements at npl and a comparison with monoenergetic data recorded at ptb," Tech. Rep. LA-UR-05-9004, Los Alamos National Laboratory, 2005.

[4] M. S. Gadd, T. D. McLean, D. T. Seagraves, R. H. Olsher, M. W. Mallett, and R. T. Devine, "Characterization and calibration of the lanl hsr-4 multi-sphere neutron spectroscopy system," Tech. Rep. LA-UR-05-8828, Los Alamos National Laboratory, 2005.

[5] Bubble Technology Industries, *BTI Automatic Reader: BDR-III User Manual*, 2009.

[6] Bubble Technology Industries, *BTI Bubble Detector Spectrometer: BDS For Low Resolution Neutron Spectroscopy Manual*, 2012.

[7] A. L. Justus, M. A. Duran, R. E. Montoya, D. T. Seagraves, J. R. Bland, and T. D. McLean, "Recent firmware and hardware upgrades to the hpi2080 pulsed neutron rem meter," in *Modern Neutron Detection: Proceedings of a Technical Meeting*, no. IAEA-TECDOC–1935, (Vienna, Austria), pp. 167–175, IAEA, Dec. 2020.

[8] Health Physics Instruments, *Operations and Repair Manual: Model 2080B Pulse Neutron Survey Meter*, Aug. 2015.

[9] C. Moss, S. Gonzales, W. Myers, M. Nelson, R. Rothrock, S. Salazar, E. Sorensen, and G. Sundby, "Revised SNAP III Training Manual," Tech. Rep. LA-UR-17-30627, Los Alamos National Laboratory, Nov. 2017.

[10] R. McConn Jr., C. Gesh, R. Pagh, R. Rucker, and R. Williams III, "Compendium of material composition data for radiation transport modeling," Tech. Rep. PNNL-15870 Rev. 1, PNNL, 2011.

Appendices

A Neutron Flux in Lethargy Space

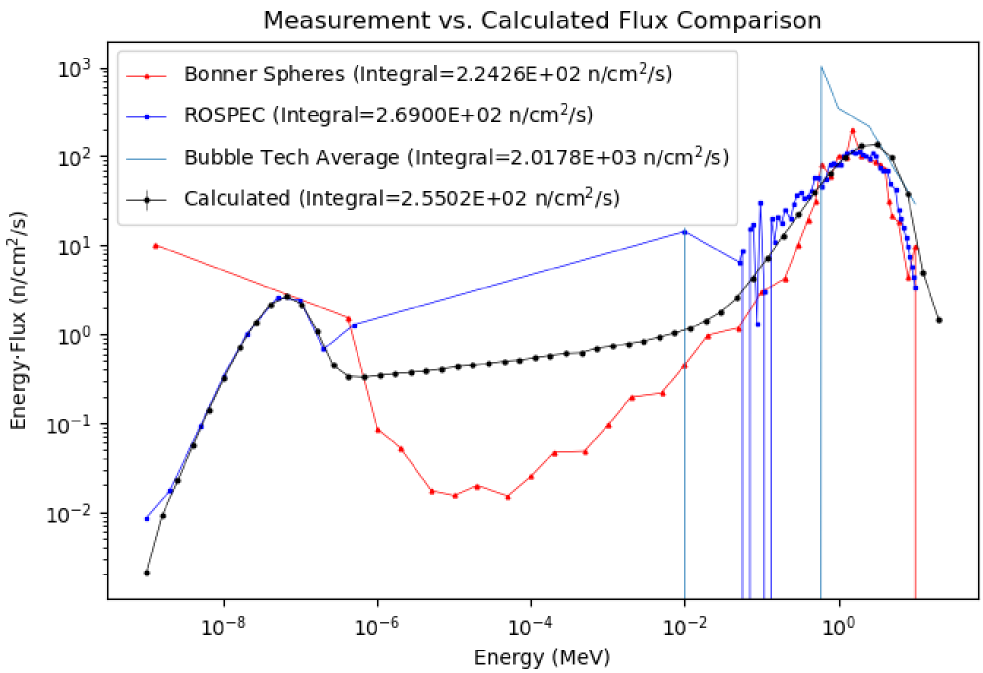

Figure 9: Measured and calculated energy differential neutron lethargy comparison at 50 cm from the source.

B ROSPEC Operating Notes

Notes on the ROSPEC unfolding code T. McLean (RP-SVS) 5/7/21

Introduction:

This document describes the code used by ROSPEC to unfold the recorded pulse height data. A brief historical background is given followed by an overview of the unfolding code and a step-by-step guide to unfolding ROSPEC data.

Historical background:

The origins of ROSPEC date back to the mid 1960's at AWRE (now AWE) in the United Kingdom. At that time, efforts lead by P.W. Benjamin and C.D Kemshall drove the development of proton recoil counters and the unfolding code required to analyze the counter's pulse height data[1,2]. The counters used on the modern version of ROSPEC are based on the original Benjamin design. Likewise, ROSPEC's unfolding code has been largely adapted from AWRE's original code.

AWRE's unfolding code (named SPEC4) is based on a sequential stripping technique that extends from the highest pulse height channel of interest to the lowest. The upper channel corresponds to the pulse height produced by the highest energy recoil proton that can be stopped in the counter — a function of counter diameter and gas fill. The bottom channel of interest is determined by interference from overlapping gamma-induced pulse heights. The overall result is a ROI that nominally extends from channels 60 to 200 for ROSPEC's proton recoil counters (each of which has a 256 channel spectrum).

The only significant changes to AWRE's SPEC4 code (even the name was retained) when adapted for ROSPEC was to extend the code to unfold four counters sequentially (the AWRE code considered a single counter only) and the additional code required to process the ^{3}He counters.

Unfolding code overview:

The SPEC4 unfolding code is briefly summarized in the following bullets.

- Either the present pulse height spectrum or a previously stored spectrum can be recalled to be unfolded.
- The user is given the option of subtracting a stored background spectrum.
- The code opens and reads an ASCII file called ZTABLES.SP4 which contains:
  - Proton range data in Hydrogen and Methane as function of neutron energy for P=1atm.
  - Counter properties including:
    - Dimensions, gas fill and pressure, spectral resolution, upper and lower boundaries for the ROI, and the linear energy calibration coefficients[3].
  - Several empirically determined correction factors that modify the calculated response functions

---

[1] PW Benjamin, CD Kemshall, J Redfearn, AWRE Report # NR 1/64, "A high-resolution spherical proportional counter", 1964

[2] PW Benjamin, CD Kemshall, A Brickstock, AWRE Report #O 9/68. "The analysis of Recoil Proton Spectra", 1968

[3] The energy calibration of each counter was established using monoenergetic neutron fields in Canada and Europe (NPL and PTB).

- For each of the four proton recoil counters, starting with the highest energy counter, i.e., CTR#3:
- User is prompted for a high-energy spectrum, if applicable, in order to take account of spectral counts caused by neutrons > 5MeV.
- The code generates energy bins by typically summing 4–6 consecutive channels. This results in the creation of 12–15 bins per counter depending on the counter's ROI and resolution.
- The code calculates the number of hydrogen atoms per cm^3 in the counter based on the data in the ZTABLES.SP4 files.
- The np elastic cross-section is calculated at the midpoint energy of each energy bin using hardwired expression.
- The proton range is calculated for each energy bin.
- A response matrix is generated taking into account incomplete energy deposition resulting from wall effects.
- The contribution to the pulse height spectrum from high-energy neutrons is calculated and subtracted on a channel-by-channel basis.
- The remaining pulse height data are differentiated by calculating the slope of the count distribution within each energy bin.
- Similarly, the response matrix is also differentiated prior to unfolding the differentiated spectrum.
- The code proceeds by applying the response function matrix sequentially starting with the highest energy bin and finishing with the lowest bin.
- The code then moves on to unfold the remaining counters (CTR#2, CTR#1, and CTR#0). In each case, counts caused by interactions with higher energy neutrons (including data from previously unfolded counters + the high energy input spectrum) are subtracted prior to applying the counter's response function.
- Following the unfolding of the CTR#0, the data from the two ^3He counters are analyzed and dosimetric quantities calculated based on the ROSPEC spectrum (thermal – 5 MeV).
- Finally, a provision to include the high-energy input spectrum in the total fluence and dose is given.

Notes:

1. It was claimed by the SPEC4 code developers that differentiating the data and the response functions minimized the propagation of errors inherent in a sequential unfolding algorithm. Though probably true, quite often — especially when relatively few counts are collected — the unfolded spectrum will demonstrate spectral structure in the lower energy bins (< 300 keV) that is inconsistent with the counter's resolution. In some extreme cases, bins with a negative fluence are possible (the code has no provision to prevent this), invariably the next lowest energy bin will have a relatively high fluence as a result of the sequential unfolding process. However, in general, fluence is conserved — it's just not always distributed correctly. The saving grace is that neutron dose coefficients are relatively small and vary smoothly over this energy region and therefore the integrated dose is fairly insensitive as to how fluence is allocated by the code.

2. The unfolding code does not include an uncertainty analysis. Independent assessments of ROSPEC performance in neutron reference fields have usually shown agreement well within ±10% of the conventionally true dose rate[4,5,6].

---

[4] J Atanackovic et al, NIM, A774,6,2015
[5] RB Schwartz, CM Eisenhauer, Radiat. Prot. Dosim., 55(2), 99, 1994
[6] W Rosenstock et al, Radiat. Prot. Dosim., 70(1-4), 290, 1997

Step-by-step unfolding of ROSPEC data:

1. The current ROSPEC pulse height spectrum or a previously stored spectrum (*File -> OpenData*) can be recalled for unfolding (Fig. 1).

2. The unfolding process is initiated as shown in Fig. 2. The unfolding code is a FORTRAN program (ZSPEC4.EXE), which is "spawned" by the ROSPEC software. It opens in a new DOS window as shown in Fig. 3.

3. The user is first prompted for a filename to store the results. I always chose the default option, i.e., *"Enter"* — perhaps because this feature does not seem to work! The default option creates a filename called UNFOLD.*** where *** represents several output files with differing suffixes (the DOS convention for file names is in force, i.e., 8+3 characters).

4. Next, an option to subtract a previously stored background is presented. Typically, the count rates during a measurement are much higher than the background rates — so I do not bother. But if desired, a spectrum can be stored as a background spectrum using the *Tools -> Create bkg file* menu option.

5. The code proceeds to open and read the ZTABLES.SP4 file stored in the ROSPEC/SPEC4 folder

6. The code then begins to unfold the SP6 (CTR#3) pulse height spectrum and the user is prompted for a high-energy input spectrum, i.e., for E>5 MeV. The options are:

    a. U: user manually enters the high energy spectrum as E(MeV), lethargy data pairs
    b. P: let the program use the high-energy spectrum calculated so far (which is non-existent for the SP6 counter). The "P" option is appropriate when no high-energy spectrum is necessary, e.g. unfolding an AmLi spectrum.
    c. F: read the input spectrum from a stored text file.
    d. Q: to quit and return to ROSPEC program

7. The ROSPEC data shown in Fig. 1 was collected using a bare Cf source, so option "F" is appropriate in this case. The user is then prompted for the filename with the high-energy spectrum. ROSPEC has two such files: FISINPUT, which is a generic spontaneous fission spectrum, and AMBE for unfolding AmBe spectra. Note that if no filename is entered, the code will look for a file called SSS.TMP, which is created during the unfolding of SSS (Simple Scintillation Spectrometer) data. The SSS is ROSPEC's high-energy complement instrument.

8. The code then calculates a scaling or normalization factor to seamlessly merge the high-energy spectrum with the upper end of the SP6 spectrum. The user has the option of ignoring this factor and entering a different value. The option to change the scaling factor is always declined.

9. All the information the code requires to unfold the SP6 spectrum is now provided. The code then presents the unfolded spectrum as shown in Fig. 3. It then proceeds to unfold the remaining counters in order of decreasing energy. The appropriate response to the input spectrum question is now the "P" option, i.e., use the unfolded spectral data calculated so far.

10. The program calculates and prints the overlap factor, which is a measure of the spectral agreement between adjacent counters. Values of 0.80–1.00 are considered typical – as highlighted and/or circled in Fig. 3.

11. After the last proton recoil counter is unfolded (SP2-1 aka CTR#0) the code analyzes the data from the ^{3}He counters. The ^{3}He analysis is based on thermal peak counts in CTR#4 and #5 to calculate the thermal an epi-thermal fluence respectively. The factors to convert count rate to fluence rate where determined using a thermal neutron column at GKSS (Hamburg) for CTR#4 and empirically for CTR#5.

12. The code then prints fluence and dosimetric data based on the ROSPEC data. An option to include the high-energy spectrum is offered and, if accepted, the code will print the combined spectrum and dose.

13. Pressing any key will exit the unfolding code and return the user to the ROSPEC program.

14. To display the unfolded spectrum, from the ROSPEC GUI select *Display > Unfolded|Smoothed* from the menu toolbar (Fig. 4). The first spectrum shows the individual neutron spectra from each of the proton recoil counters in lethargy format. Pressing any key will display the smoothed spectrum for these counters.

15. To display the combined spectrum, select the *ROSPEC thermal-4.5MeV* option under the *Display* menu (Fig. 4). This spectrum will include the high-energy input spectrum, if so selected in step 12.

16. All the data (and more) presented during the unfolding process is written to text files in the ROSPEC folder. Fig. 8 is a directory listing of the files written by the unfolding code. The more useful of these files are listed below:

    a. UNFOLD.DAT — echoes the unfolding output, i.e., the output shown in Fig. 3. This is an ASCII file but misidentified as a PDF in Fig.8
    b. MERGE.SPM — contains the ROSPEC + high-energy input spectrum and dosimetric data
    c. TOTAL.PLT — contains the unfolded spectrum in terms of lethargy in a histogram format for ease of plotting.

Figure 1. ROSPEC GUI

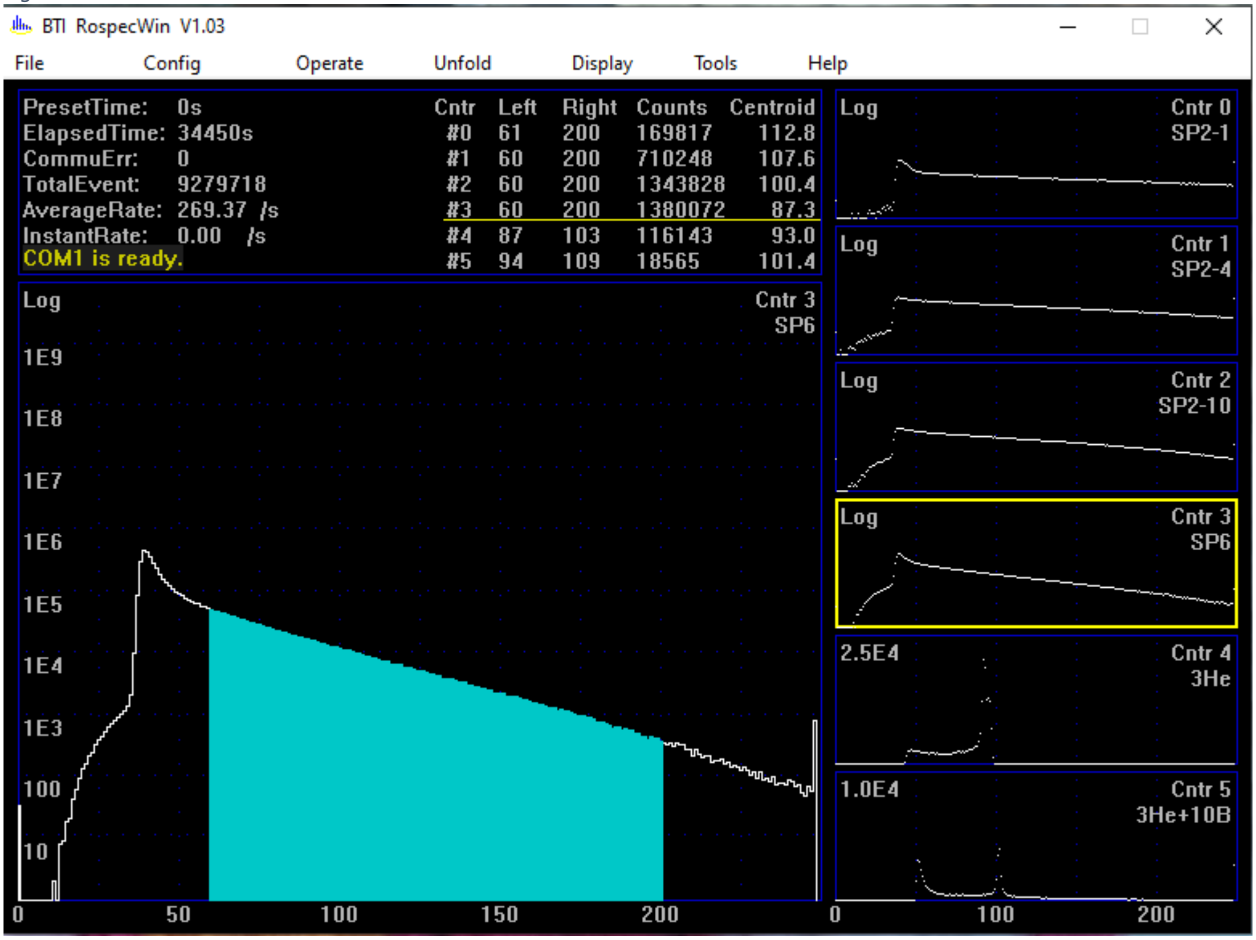

Figure 2. Initiate unfolding of ROSPEC data

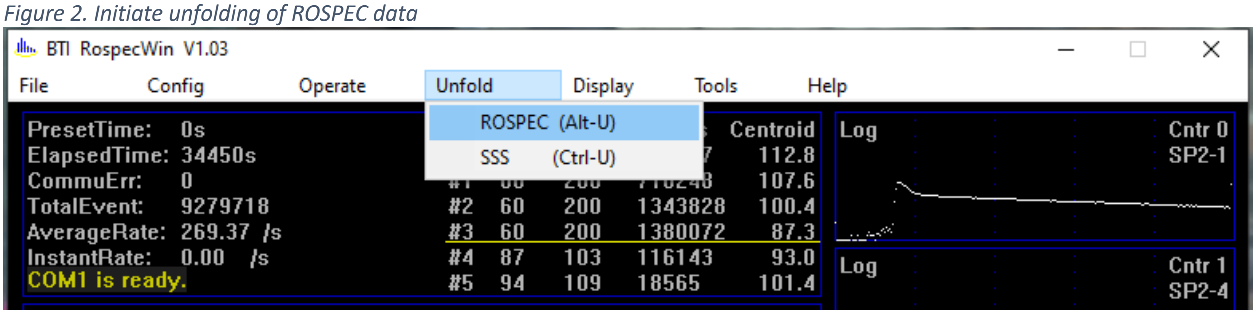

Figure 3. Screenshot of unfolding code

```
C:\WINDOWS\system32\cmd.exe

            SPEC4 Program   (v 7.18)


  Enter filename to store results:
  Spectrum will be saved in file: UNFOLD.spm
On-line analyis
 Unfolded data stored in file UNFOLD.DAT


  Do you wish to subtract background data stored in
  file C:\ROSPEC\SPEC4\ZSPEC4.BKG from current
  spectrum ? (Y or N) n

 Background will not be subtracted from data


ZTABLES.SP4 FOR LANL2:   calibrated Oct.11 2001. New range & CFE,CFS data. New S
□EMAX = 5.250  BBIAS =-16.3  CAL =0.02550  UFLXMIN = 1.350  UFLXMAX = 5.250
Enter U (user) or P (program) or F(file) for input spectrum or Q to quit ? f
  Enter filename for neutron spectrum:
  For SSS file, just hit <ENTER> fisinput
  Enter normalizing factor [1.00]
..................................

Overlap ratio between SP6 and input spectrum =  1.6815E+07
Use this factor to renormalize input spectrum ? (Y/n)
y
..................................
A (Ratio of intensities in overlap region):    1.000
```

```
Calculated Neutron Spectrum - SP6        scale factor:   1.0000
 Indicated       Energy       Flux /      Flux /      Flux /      Avg
  Channel       Boundary      Group        MeV       Lethargy      E.

   65   69  1.204  1.331   1.105E+06   8.664E+06   1.097E+07   1.267
   70   75  1.331  1.484   1.229E+06   8.034E+06   1.130E+07   1.408
   76   81  1.484  1.637   1.112E+06   7.269E+06   1.134E+07   1.561
   82   89  1.637  1.841   1.360E+06   6.666E+06   1.158E+07   1.739
   90   97  1.841  2.045   1.220E+06   5.978E+06   1.161E+07   1.943
   98  105  2.045  2.249   1.074E+06   5.265E+06   1.130E+07   2.147
  106  115  2.249  2.504   1.169E+06   4.585E+06   1.089E+07   2.377
  116  126  2.504  2.785   1.119E+06   3.989E+06   1.054E+07   2.644
  127  138  2.785  3.091   1.031E+06   3.368E+06   9.886E+06   2.938
  139  152  3.091  3.448   9.469E+05   2.652E+06   8.662E+06   3.269
  153  167  3.448  3.830   7.946E+05   2.077E+06   7.552E+06   3.639
  168  184  3.830  4.264   7.329E+05   1.691E+06   6.835E+06   4.047
  185  202  4.264  4.723   5.577E+05   1.215E+06   5.454E+06   4.493
  203  223  4.723  5.258   5.426E+05   1.013E+06   5.051E+06   4.990

□EMAX = 1.600  BBIAS =-16.3  CAL =0.00860  UFLXMIN = 0.400  UFLXMAX = 1.400
Enter U (user) or P (program) or F(file) for input spectrum or Q to quit ? p
..................................
A (Ratio of intensities in overlap region):    0.9484

Calculated Neutron Spectrum - SP2-10     scale factor:   1.0000
 Indicated       Energy       Flux /      Flux /      Flux /      Avg
  Channel       Boundary      Group        MeV       Lethargy      E.

   60   64  0.363  0.406   5.484E+05   1.275E+07   4.897E+06   0.384
   65   69  0.406  0.449   4.960E+05   1.154E+07   4.926E+06   0.427
   70   75  0.449  0.501   5.637E+05   1.092E+07   5.181E+06   0.475
   76   82  0.501  0.561   6.753E+05   1.122E+07   5.946E+06   0.531
   83   89  0.561  0.621   6.423E+05   1.067E+07   6.298E+06   0.591
   90   97  0.621  0.690   7.238E+05   1.052E+07   6.888E+06   0.655
   98  106  0.690  0.767   7.856E+05   1.015E+07   7.386E+06   0.728
  107  116  0.767  0.853   8.637E+05   1.004E+07   8.128E+06   0.810
  117  127  0.853  0.948   9.718E+05   1.027E+07   9.241E+06   0.900
  128  139  0.948  1.051   9.260E+05   8.973E+06   8.959E+06   0.999
  140  152  1.051  1.163   9.708E+05   8.683E+06   9.603E+06   1.107
  153  167  1.163  1.292   1.174E+06   9.104E+06   1.116E+07   1.227
  168  184  1.292  1.438   1.266E+06   8.661E+06   1.181E+07   1.365
  185  203  1.438  1.601   1.465E+06   8.965E+06   1.361E+07   1.520

□EMAX = 0.750  BBIAS =-16.7  CAL =0.00409  UFLXMIN = 0.150  UFLXMAX = 0.750
Enter U (user) or P (program) or F(file) for input spectrum or Q to quit ? p
```

```
..................................
 A (Ratio of intensities in overlap region):   0.8857

 Calculated Neutron Spectrum - SP2-4      scale factor:    1.0000
  Indicated       Energy        Flux /      Flux /       Flux /      Avg
   Channel       Boundary       Group        MeV        Lethargy      E.

    52   55  0.138  0.155   3.403E+05   2.080E+07   3.043E+06   0.146
    56   59  0.155  0.171   2.460E+05   1.503E+07   2.445E+06   0.163
    60   64  0.171  0.191   2.656E+05   1.299E+07   2.351E+06   0.181
    65   69  0.191  0.212   2.606E+05   1.274E+07   2.567E+06   0.202
    70   75  0.212  0.236   3.344E+05   1.363E+07   3.051E+06   0.224
    76   81  0.236  0.261   2.842E+05   1.158E+07   2.878E+06   0.249
    82   88  0.261  0.290   3.538E+05   1.236E+07   3.399E+06   0.275
    89   96  0.290  0.322   4.360E+05   1.332E+07   4.072E+06   0.306
    97  105  0.322  0.359   4.452E+05   1.209E+07   4.116E+06   0.341
   106  115  0.359  0.400   4.730E+05   1.157E+07   4.386E+06   0.380
   116  125  0.400  0.441   4.701E+05   1.149E+07   4.829E+06   0.420
   126  138  0.441  0.494   6.210E+05   1.168E+07   5.454E+06   0.467
   139  151  0.494  0.547   5.944E+05   1.118E+07   5.815E+06   0.521
   152  166  0.547  0.609   7.190E+05   1.172E+07   6.766E+06   0.578
   167  182  0.609  0.674   7.962E+05   1.217E+07   7.796E+06   0.641
   183  201  0.674  0.752   8.556E+05   1.101E+07   7.841E+06   0.713

 EMAX = 0.225  BBIAS =-23.6  CAL =0.00126  UFLXMIN = 0.050  UFLXMAX = 0.225
 Enter U (user) or P (program) or F(file) for input spectrum or Q to quit ? p
..................................
 A (Ratio of intensities in overlap region):   0.9434

 Calculated Neutron Spectrum - SP2-1      scale factor:    1.0000
  Indicated       Energy        Flux /      Flux /       Flux /      Avg
   Channel       Boundary       Group        MeV        Lethargy      E.

    62   65  0.046  0.052   1.247E+05   2.474E+07   1.211E+06   0.049
    66   69  0.052  0.057   8.441E+04   1.675E+07   9.046E+05   0.054
    70   75  0.057  0.064   1.127E+05   1.491E+07   8.989E+05   0.060
    76   80  0.064  0.070   9.485E+04   1.506E+07   1.012E+06   0.067
    81   86  0.070  0.078   1.105E+05   1.462E+07   1.084E+06   0.074
    87   93  0.078  0.087   1.019E+05   1.155E+07   9.507E+05   0.082
    94  101  0.087  0.097   1.051E+05   1.042E+07   9.565E+05   0.092
   102  110  0.097  0.108   8.035E+04   7.085E+06   7.260E+05   0.103
   111  119  0.108  0.120   1.099E+05   9.690E+06   1.103E+06   0.114
   120  130  0.120  0.133   2.239E+05   1.616E+07   2.042E+06   0.127
   131  141  0.133  0.147   2.336E+05   1.685E+07   2.364E+06   0.140
   142  154  0.147  0.164   8.055E+04   4.918E+06   7.639E+05   0.155
   155  169  0.164  0.183   8.484E+04   4.489E+06   7.764E+05   0.173
   170  185  0.183  0.203   2.404E+05   1.192E+07   2.295E+06   0.193
   186  203  0.203  0.225   3.151E+05   1.389E+07   2.971E+06   0.214


                       FLUENCE             FLUENCE RATE
                       (n cm-2)            (n cm-2 s-1)

 50 keV - 4.5 MeV   :  2.65E+07              7.69E+02
 Epi-thermal region :  2.59E+06              7.52E+01
 Thermal region     :  3.36E+05              9.75E+00

 TOTAL              :  2.94E+07              8.54E+02


                   DOSIMETRIC DATA

                      KERMA     NCRP-38    H*(10)        KERMA     NCRP-38    H*(10)
                      (rads)     (rem)      (Sv)       (mrads/hr) (mrem/hr) (uSv/hr)
 50keV  - 4.5 MeV   : 6.79E-02  8.33E-01  9.72E-03      7.09E+00  8.71E+01  1.02E+03
 Epi-thermal regio  : 1.80E-04  3.53E-03  3.36E-05      1.88E-02  3.69E-01  3.51E+00
 Thermal region     : 6.71E-06  3.42E-04  3.56E-06      7.02E-04  3.58E-02  3.72E-01

 TOTAL              : 6.80E-02  8.37E-01  9.75E-03      7.11E+00  8.75E+01  1.02E+03


 MERGE ROSPEC and INPUT SPECTRUM ? (Y/n) : y
  MERGED DATA STORED IN FILE C:\ROSPEC\MERGE.SPM
```

MERGED SSS/ROSPEC NEUTRON SPECTRUM :

E2 (MeV)	E1 (MeV)	FLUENCE/ GROUP	FLUENCE/ MeV	FLUENCE/ Lethargy	E avg. (MeV)
.1000E-08	.2000E-08	7.587E+02	7.587E+11	1.095E+03	.1500E-08
.2000E-08	.5000E-08	4.868E+03	1.623E+12	5.313E+03	.3500E-08
.5000E-08	.1000E-07	1.481E+04	2.961E+12	2.136E+04	.7500E-08
.1000E-07	.2000E-07	4.364E+04	4.364E+12	6.296E+04	.1500E-07
.2000E-07	.5000E-07	1.353E+05	4.510E+12	1.477E+05	.3500E-07
.5000E-07	.1000E-06	1.058E+05	2.115E+12	1.526E+05	.7500E-07
.1000E-06	.2000E-06	2.974E+04	2.974E+11	4.291E+04	.1500E-06
.2000E-06	.5000E-06	8.254E+04	2.751E+11	9.008E+04	.3500E-06
.5000E-06	.1000E-01	1.873E+06	1.873E+08	1.891E+05	.5000E-02
.1000E-01	.5153E-01	6.339E+05	1.526E+07	3.866E+05	.3077E-01
.5153E-01	.5657E-01	8.441E+04	1.675E+07	9.046E+05	.5405E-01
.5657E-01	.6413E-01	1.127E+05	1.491E+07	8.989E+05	.6035E-01
.6413E-01	.7043E-01	9.485E+04	1.506E+07	1.012E+06	.6728E-01
.7043E-01	.7799E-01	1.105E+05	1.462E+07	1.084E+06	.7421E-01
.7799E-01	.8681E-01	1.019E+05	1.155E+07	9.507E+05	.8240E-01
.8681E-01	.9689E-01	1.051E+05	1.042E+07	9.565E+05	.9185E-01
.9689E-01	.1082E+00	8.035E+04	7.085E+06	7.260E+05	.1026E+00
.1082E+00	.1196E+00	1.099E+05	9.690E+06	1.103E+06	.1139E+00
.1196E+00	.1334E+00	2.239E+05	1.616E+07	2.042E+06	.1265E+00
.1334E+00	.1473E+00	2.336E+05	1.685E+07	2.364E+06	.1404E+00
.1473E+00	.1637E+00	8.055E+04	4.918E+06	7.639E+05	.1555E+00
.1637E+00	.1826E+00	1.729E+05	9.146E+06	1.582E+06	.1731E+00
.1826E+00	.2027E+00	2.497E+05	1.238E+07	2.384E+06	.1927E+00
.2027E+00	.2364E+00	4.477E+05	1.330E+07	2.914E+06	.2196E+00
.2364E+00	.2609E+00	2.842E+05	1.158E+07	2.878E+06	.2487E+00
.2609E+00	.2896E+00	3.538E+05	1.236E+07	3.399E+06	.2753E+00
.2896E+00	.3223E+00	4.360E+05	1.332E+07	4.072E+06	.3059E+00
.3223E+00	.3591E+00	4.452E+05	1.209E+07	4.116E+06	.3407E+00
.3591E+00	.4000E+00	4.730E+05	1.157E+07	4.386E+06	.3796E+00
.4000E+00	.4409E+00	4.746E+05	1.160E+07	4.875E+06	.4205E+00
.4409E+00	.4941E+00	6.032E+05	1.135E+07	5.298E+06	.4675E+00
.4941E+00	.5472E+00	5.963E+05	1.122E+07	5.834E+06	.5207E+00
.5472E+00	.6086E+00	6.900E+05	1.125E+07	6.494E+06	.5779E+00
.6086E+00	.6740E+00	7.442E+05	1.137E+07	7.286E+06	.6413E+00
.6740E+00	.7671E+00	9.784E+05	1.051E+07	7.563E+06	.7206E+00
.7671E+00	.8531E+00	8.637E+05	1.004E+07	8.128E+06	.8101E+00
.8531E+00	.9477E+00	9.718E+05	1.027E+07	9.241E+06	.9004E+00
.9477E+00	.1051E+01	9.260E+05	8.973E+06	8.959E+06	.9993E+00
.1051E+01	.1163E+01	9.708E+05	8.683E+06	9.603E+06	.1107E+01
.1163E+01	.1292E+01	1.174E+06	9.104E+06	1.116E+07	.1227E+01
.1292E+01	.1484E+01	1.640E+06	8.523E+06	1.181E+07	.1388E+01
.1484E+01	.1637E+01	1.112E+06	7.269E+06	1.134E+07	.1561E+01
.1637E+01	.1841E+01	1.360E+06	6.666E+06	1.158E+07	.1739E+01
.1841E+01	.2045E+01	1.220E+06	5.978E+06	1.161E+07	.1943E+01
.2045E+01	.2249E+01	1.074E+06	5.265E+06	1.130E+07	.2147E+01
.2249E+01	.2504E+01	1.169E+06	4.585E+06	1.089E+07	.2377E+01
.2504E+01	.2785E+01	1.119E+06	3.989E+06	1.054E+07	.2644E+01
.2785E+01	.3091E+01	1.031E+06	3.368E+06	9.886E+06	.2938E+01
.3091E+01	.3448E+01	9.469E+05	2.652E+06	8.662E+06	.3269E+01
.3448E+01	.3830E+01	7.946E+05	2.077E+06	7.552E+06	.3639E+01
.3830E+01	.4264E+01	7.329E+05	1.691E+06	6.835E+06	.4047E+01
.4264E+01	.4723E+01	5.316E+05	1.158E+06	5.200E+06	.4493E+01
.4723E+01	.5500E+01	6.986E+05	8.986E+05	4.584E+06	.5111E+01
.5500E+01	.6000E+01	2.616E+05	5.232E+05	3.007E+06	.5750E+01
.6000E+01	.6500E+01	1.929E+05	3.857E+05	2.410E+06	.6250E+01
.6500E+01	.7000E+01	1.416E+05	2.831E+05	1.910E+06	.6750E+01
.7000E+01	.7500E+01	1.036E+05	2.072E+05	1.502E+06	.7250E+01
.7500E+01	.8000E+01	7.553E+04	1.511E+05	1.170E+06	.7750E+01
.8000E+01	.8500E+01	5.495E+04	1.099E+05	9.064E+05	.8250E+01
.8500E+01	.9000E+01	3.989E+04	7.977E+04	6.978E+05	.8750E+01
.9000E+01	.9500E+01	2.891E+04	5.782E+04	5.347E+05	.9250E+01
.9500E+01	.1000E+02	2.096E+04	4.192E+04	4.086E+05	.9750E+01

INTEGRATED FLUENCE = 3.0466E+07   FLUENCE RATE = 8.8435E+02

		INTEGRATED DOSE	DOSE RATE
KERMA		= 7.1418E-02 rads	7.4631E+00 mrads/hr
H	NCRP-38	= 8.7046E-01 rem	9.0963E+01 mrem/hr
H*(10)	ICRP-74	= 1.0088E-02 Sv	1.0541E+03 uSv/hr
Hp(10,0)	ICRP-74	= 1.0457E-02 Sv	1.0928E+03 uSv/hr

Figure 4. Display of unfolded spectrum

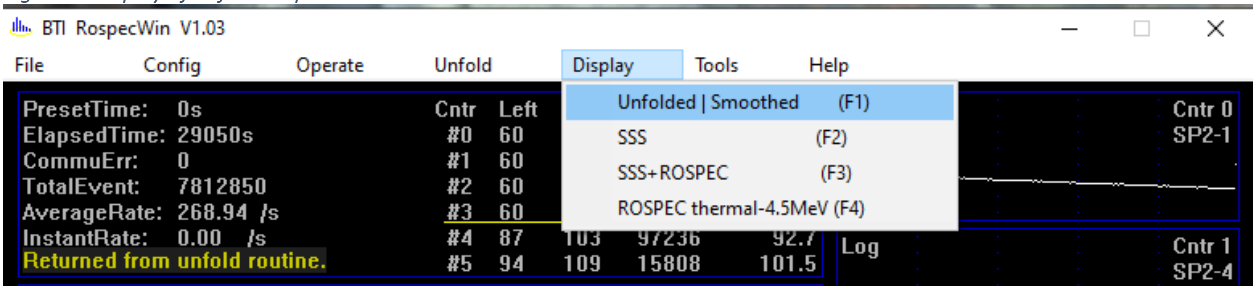

Figure 5. Lethargy plots of the four proton recoil counters

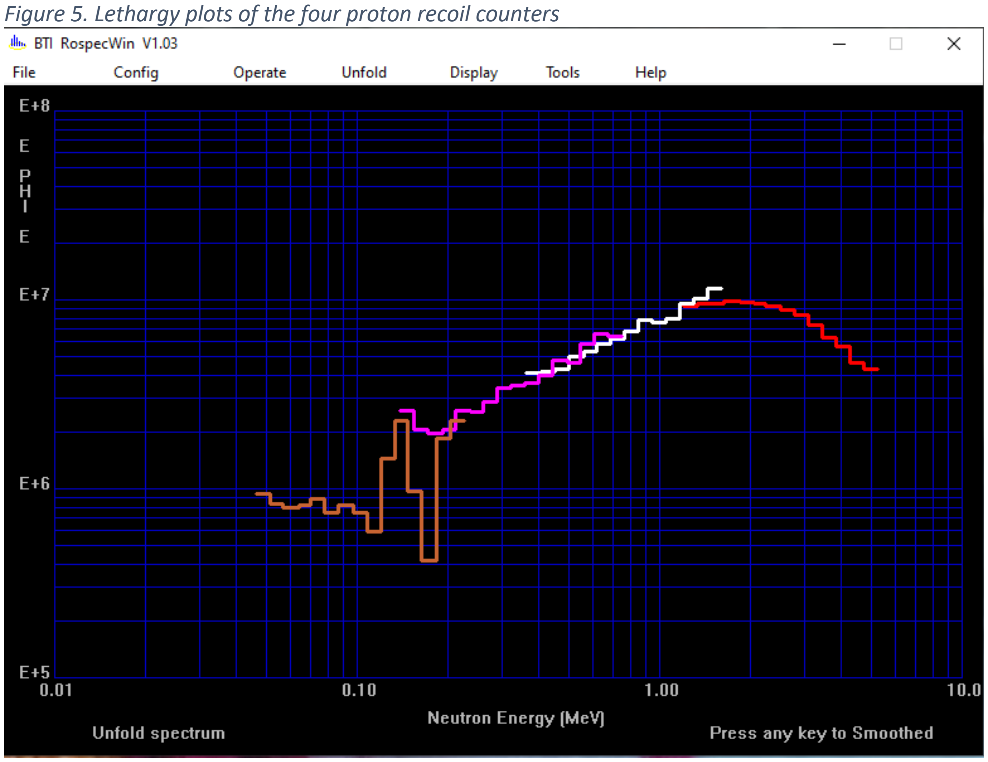

Figure 6. Smoothed neutron spectrum for the recoil proton counters

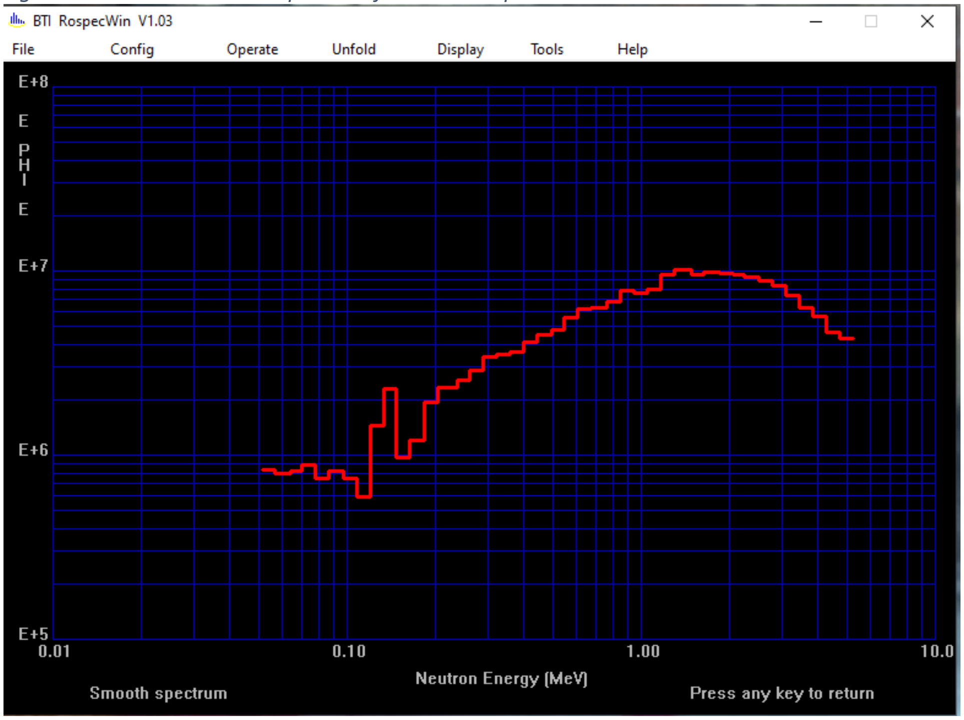

Figure 7. Overall neutron spectrum in Lethargy format

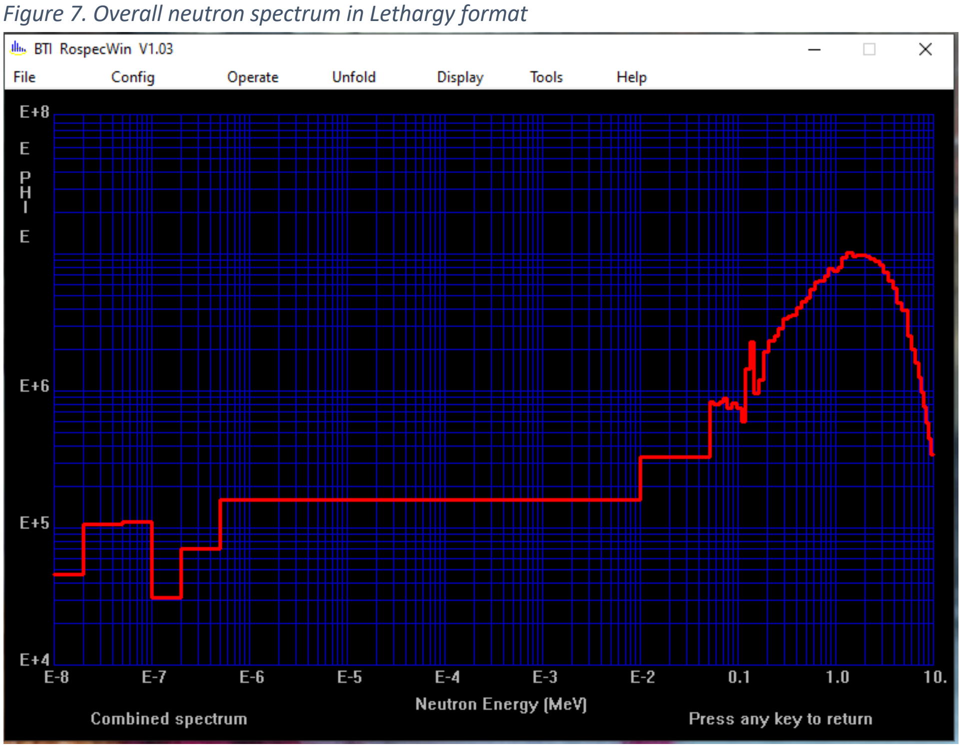

Figure 8. Files created during unfolding

Name	Date modified	Type	Size
dose	5/6/2021 8:49 AM	OUT File	3 KB
BSS.IN	5/6/2021 8:49 AM	IN File	4 KB
combined	5/6/2021 8:49 AM	PLT File	5 KB
merge	5/6/2021 8:49 AM	PLT File	4 KB
merge	5/6/2021 8:49 AM	SPM File	6 KB
Smooth	5/6/2021 8:49 AM	PLT File	4 KB
spectrum	5/6/2021 8:49 AM	INP File	3 KB
total	5/6/2021 8:49 AM	PLT File	5 KB
unfold	5/6/2021 8:49 AM	Adobe Acrobat D...	7 KB
unfold	5/6/2021 8:49 AM	PLT File	5 KB
UNFOLD	5/6/2021 8:49 AM	SPM File	12 KB
fort.10	5/6/2021 8:49 AM	10 File	1 KB
summary.3He	5/6/2021 8:49 AM	3HE File	1 KB
UNFOLD	5/6/2021 8:49 AM	SPT File	26 KB
YCH	5/6/2021 8:49 AM	Adobe Acrobat D...	5 KB

C Bonner Sphere Operating Notes

Guidance on use of Bonner Spheres rev.1 4/2021

Assembling the spheres

The Bonner spheres are packed in two Pelican cases. The lighter one contains the 3-, 3.5-, 4-, 4.5-, and 5-inch diameter spheres along with all the electronics including the counters needed for operation. The heavier case contains the 6-, 7-, 8-, 10-, and 12-inch diameter spheres.

The spheres sit on dedicated "coffee cans" whose heights are such that the centers of the spheres are always at the same height. The 3–8-inch spheres are held in place with spring loaded wires — though the 8 inch is currently detached. The 10- and 12-inch spheres are not secured in this fashion. The bottom of each can sits on a base - the larger spheres have bases, which are in two pieces — but as all components ("coffee cans," base plates, etc..) are labelled with the corresponding sphere diameter — they should be easily assembled. Note that the base of the 7-inch sphere is slightly warped. When carrying, hold the sphere assembly with one hand beneath the base plate to prevent accidental decoupling.

We have included a tripod — its use is optional, but we have included a circular plate (probably more than one) that can be screwed onto the tripod and which nicely fits the base plates. I would recommend a C-clamp or other clamp (not included) to secure the base to the plate.

Two counters are included labeled as "e" and "f" on the end cap. The idea is that while one sphere is the neutron field, another sphere with the other counter can be prepped for the next run. The counters have very similar sensitivities and can be used interchangeably. Though I would recommend at least one count with both counters using the same sphere and measurement configuration.

The counters are inserted in the spheres using (1) a threaded two piece cylindrical cap for the spherical end of the counter (common to all spheres), (2) PE spacers that surround the stem of the counter, and (3) a threaded retaining ring (common to all spheres). The smaller diameter spheres are very straightforward to use and I would recommend starting with them. All the spacers are marked with their sphere diameters just in case they get mixed up. Though having designated disassembly and assembly areas should eliminate that possibility. Always a good idea to reassemble the sphere with its associated bits and bobs immediately after usage. The larger spheres, (i.e., where the sphere radius is greater than the length of the counter stem) are the most tricky and they must be assembled in the right order. This includes making sure the cylindrical PE cap is placed first and that the retaining ring is on the HV/signal cable before attaching it to the counter. It's all straightforward and obvious once assembled, though it may require some trial and error to get the choreography correct. Also note that some of the spacers are a tight fit (e.g., the 7-inch assembly) and may require an optimal orientation of the spacers and squeezing them together as you insert the counter assembly. It may also require some effort to remove the counter assembly after a run — using the counter's stem to pull out the assembly should do the trick.

We orientate the sphere so that counter's stem is 180 degrees with respect to the source.

Figure 1. Sphere on tripod.

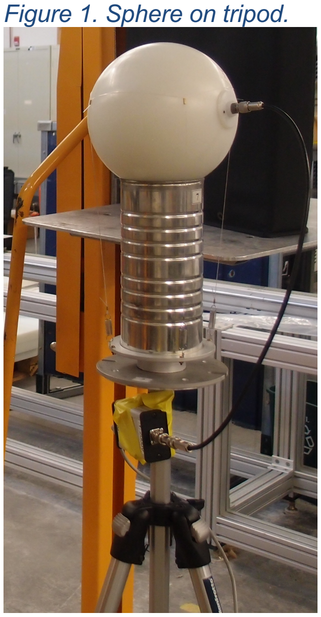

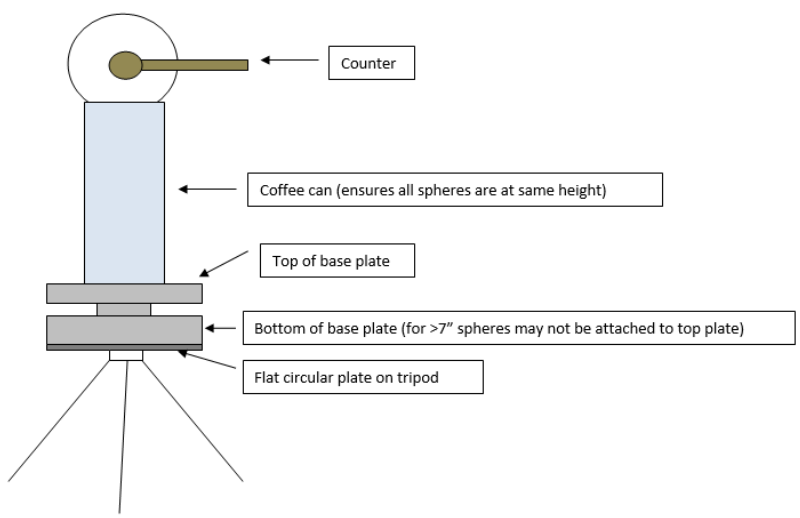

A run with the bare counter is also required. We have included at least two stands to facilitate positioning a bare counter. This is the only measurement that needs a background count — though it's probably going to be negligible.

Measurements made at center-to-center distances closer than 50 cm will probably require a geometry correction factor — especially for the larger spheres. These factors can be generated with MCNP.

It is not a rigorous requirement that count rate data be collected with every sphere. However, it is always better to acquire as much data as possible.

<u>Electronics assembly</u>

The diagrams below show how to connect a counter to your laptop. There are two options. There's a simple option if local monitoring is feasible or USB extender boxes (no drivers are required, I think) can be used if remote operation is required. Both options use a Quaesta module that provides the HV and MCA. We have included two modules for redundancy, but we have relied exclusively on SN #002 lately. We have also provided two signal/HV cables for connecting the counter to the Quaesta module in case one should fail. The USB cables and a long CAT-5 cable have also been included.

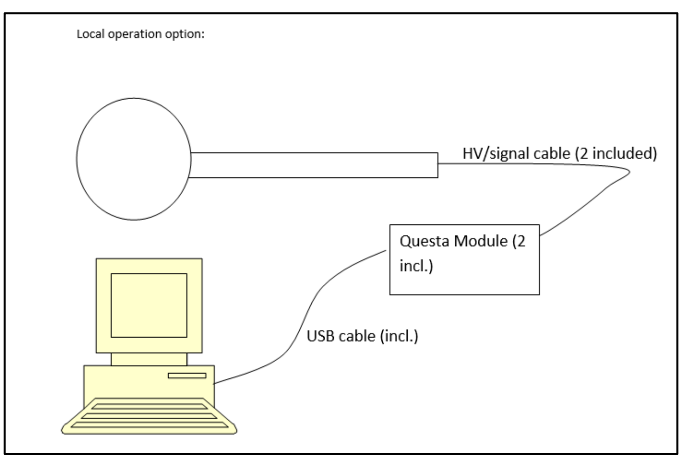

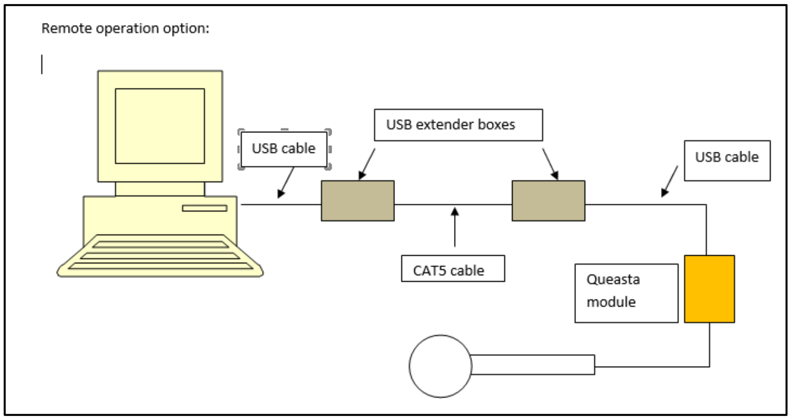

The HV/signal cable should be attached finger tight to the counter. We have found that if over tightened, the nut at the end of the counter will come loose before the cable during disassembly. On the other hand, if not tight enough, there may be some noise in the bottommost channel of the pulse height spectrum.

As shown in the figure above, we tape the Quaesta module to the tripod.

Operating software

The operating software is included on a thumb drive which is in one of the bags that contain one of the Quaesta modules. The application (BSS7.EXE) was written in Python and all the auxiliary files required to run it as a standalone program have been included. It is fairly rudimentary but is hopefully easy to use. A screen shot is shown below.

- Text boxes are provided to enter info such as sphere diameter, counter ID and a description of the measurement. All this data is automatically stored at the end of every run in a file named BSS.dat. Though, of course, it's prudent to manually record the important data as well.

- The operating HV has been preset at 1250 V and the gain at 20 (at least in Quaesta module #002) and should not need adjusting. The applied voltage should never exceed 1300 V (despite what is indicated in the screenshot).

The pulse height spectrum should extend as far as about channel 50 under these conditions.

- A finite run time can be entered or a value of "0" seconds to give a run that continues until the Stop button is pressed.

- ROI markers delineate the gamma and the neutron regions as indicated in the upper right hand corner of the display. Typically they don't need adjusting. The number of counts and the average count rate in each ROI are also displayed in this display area. At the end of each run, the spectrum counts and ROI count rates are automatically appended to the BSS.dat file.

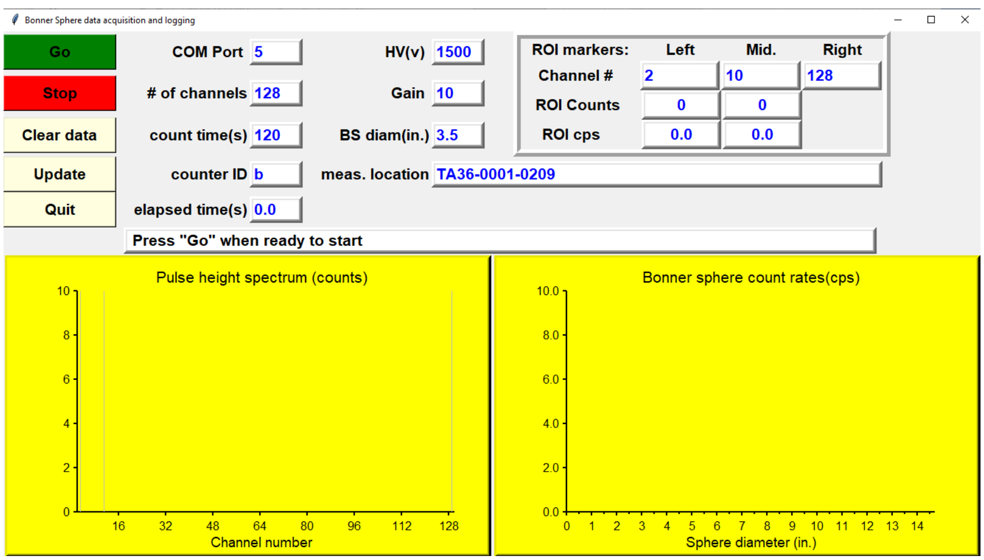

- Select "Go" to start a run. The software will automatic locate the correct COM port and initiate a small delay while the HV ramps up. At the end of the run, the HV will automatically turn off. The count rate display in the lower right hand corner will update based on the sphere diameter and neutron count rate. For a ^{252}Cf source, the maximum count rate will typically be observed for the 7-inch counter. Regardless, the count rates should vary in a smooth manner with sphere diameter.

- Select "Stop" to manually stop a run — the accumulated data will be stored.

- Select "Clear data" if you want to restart a run mid count. Note that while collecting data the software may be sluggish to respond.

Measurement notes

- A minimum distance of 50 cm from the source to sphere center should be maintained to avoid having to introduce geometry correction factors.

- Though a finite run time can be entered — the software will typically overrun by 1 or 2 seconds. I would recommend at least 3 or 4 minutes of count time per sphere to reduce any timing errors and, if possible, and if time allows, >5000 neutron ROI counts.

- The Quaesta's minimum dead time per count is 40 µs. So observed count rates of 250 cps imply a 1% dead time correction, i.e., a true count rate of 252.5 cps.